Various Crystalline Morphology of Poly(butylene Succinate-*co*-butylene Adipate) in Its Miscible Blends with Poly(vinylidene Fluoride)

Zhaobin Qiu,*,†,‡ Chunzhu Yan,† Jiaoming Lu,† Wantai Yang,† Takayuki Ikehara,§ and Toshio Nishi||

State Key Laboratory of Chemical Resource Engineering, Beijing University of Chemical Technology, Beijing 100029, China, The Key Laboratory of Beijing City on Preparation and Processing of Novel Polymer Materials, Beijing University of Chemical Technology, Beijing 100029, China, Department of Applied Chemistry, Faculty of Engineering, Kanagawa University, 3-27-1, Rokkakubashi, Kanagawa-ku, Yokohama 221-8686, Japan, and Department of Organic and Polymeric Materials, Graduate School of Science and Engineering, Tokyo Institute of Technology, 2-12-1 Ohokayama, Meguro-ku, Tokyo 152-8552, Japan

Received: November 16, 2006; In Final Form: January 8, 2007

Poly(vinylidene fluoride) (PVDF) and poly(butylene succinate-*co*-butylene adipate) (PBSA) are crystalline/crystalline polymer blends with PVDF being the high-T_m component and PBSA being the low-T_m component, respectively. PVDF/PBSA blends are miscible as shown by the decrease of crystallization peak temperature and melting point temperature of each component with increasing the other component content and the homogeneous melt. The low-T_m component PBSA presents various confined crystalline morphologies due to the presence of the high-T_m component PVDF crystals by changing blend composition and crystallization conditions in the blends. There are mainly three different types of crystalline morphologies for PBSA in its miscible blends with PVDF. First, crystallization of PBSA commenced in the interspherulitic regions of the PVDF spherulites and continued to develop inside them in the case of PVDF-rich blends under two-step crystallization conditions. Second, PBSA spherulites appeared first in the left space after the complete crystallization of PVDF, contacted and penetrated the PVDF spherulites by forming interpenetrated spherulites in the case of PVDF-poor blends under two-step crystallization condition. Third, PBSA spherulites nucleated and continued to grow inside the PVDF spherulites that had already filled the whole space during the quenching process in the case of PBSA-rich blends under one-step crystallization condition. The conditions of forming the various crystalline morphologies were discussed.

Introduction

Miscible crystalline/crystalline polymer blends have received much less attention than fully amorphous or amorphous/crystalline systems; however, they may provide various conditions to study the crystallization behavior and morphology of polymer blends.[1−16] The difference in the melting point (T_m) of the two components has a significant influence on the crystallization kinetics and morphology when binary miscible crystalline/crystalline polymer blends crystallize from the homogeneous melt. The high-T_m component usually crystallizes first, whose spherulites almost fill the whole space, when the T_m difference is very large. In such cases, confined crystallization of the low-T_m component occurs subsequently in the spatially limited regions inside the spherulites or on the interspherulitic boarders of the high-T_m component on lowering the crystallization temperature (T_c), which are confirmed by the increase in the brightness of the spherulites.[5,6] However, two components can crystallize simultaneously depending on blend composition and crystallization temperature when the T_m difference is small.[7−14] Furthermore, interpenetrated spherulites are occasionally formed in a few miscible pairs of two crystalline polymers when the two components crystallize simultaneously.[7−14] Spherulites of one component continue to grow in the spherulites of the other component after they contact with each other. The interpenetrated spherulites formation processes have been found in poly(3-hydroxybutyrate) (PHB)/poly(L-lactide) (PLLA),[7] poly(butylene succinate) (PBSU)/poly(vinylidene chloride-*co*-vinyl chloride) (PVDCVC),[8−10] poly(ester carbonate) (PEC)/PLLA,[11,12] poly(ethylene succinate) (PES)/poly(ethylene oxide) (PEO) blends,[13] and PBSA/PEO blends.[14] The important factors in realizing interpenetrated spherulites are the difference in the lamella population density in the different spherulites of the two components, the sufficient amount of the melt of one component inside the spherulites of the other component, and the simultaneous spherulitic growth of both components.

The crystallization and morphology of binary miscible crystalline polymer blends are far away from being really understood till now. In particular, less attention has been paid to the crystallization and morphology of the low-T_m component, which are affected not only by blend composition and crystallization conditions but also strongly by the pre-existing crystals of the high-T_m component in the blends. In this work we chose PVDF and PBSA as the model blend system. The two polymers are both crystalline in their neat state, which undergo crystallization over a wide range of temperature. Since the difference in T_ms between PVDF (ca. 165 °C) and PBSA (ca. 95 °C) is

* To whom correspondence should be addressed. E-mail: qiuzb@buct.edu.cn. Fax: +86-10-64413161.

† State Key Laboratory of Chemical Resource Engineering, Beijing University of Chemical Technology.

‡ The Key Laboratory of Beijing City on Preparation and Processing of Novel Polymer Materials, Beijing University of Chemical Technology.

§ Kanagawa University.

|| Tokyo Institute of Technology.

10.1021/jp067606f CCC: $37.00
Published on Web 02/27/2007

large, the simultaneous crystallization of the two components is impossible. The crystallization of PVDF corresponds to the transition from the fully amorphous to the amorphous/semicrystalline state. PBSA is still in the melt as an amorphous diluent throughout the crystallization of PVDF. On further lowering crystallization temperature, the crystallization of PBSA corresponds to the transition from the amorphous/semicrystalline to semicrystalline/semicrystalline state. PVDF always crystallizes during the quenching process before the crystallization temperature (T_c) of PBSA is reached, and PBSA crystallizes in the matrix of the pre-existing PVDF crystals.

The crystalline morphology of PBSA in the presence of the pre-existing PVDF crystals was studied by OM. The effects of blend composition and crystallization conditions of the high-T_m component on the confined crystallization of the low-T_m component were investigated in detail. Three different types of crystalline morphologies of PBSA were found. The conditions of forming such morphologies were discussed.

Experimental Section

PVDF and PBSA were purchased from Polysciences, Inc., and Aldrich Chemical Co. Inc., respectively, and used as received. PVDF/PBSA blends were prepared with mutual solvent *N*,*N*-dimethylformamide. The solution of both polymers (0.02 g/mL) was cast on glass plate at an elevated temperature. The solvent was continued to evaporate in a controlled air stream for 1 day. The resulting films were further dried in vacuum at 50 °C for 3 days to remove the solvent completely. PVDF/PBSA blends were thus prepared with various compositions ranging from 100/0, 80/20, 65/35, 50/50, 35/65, 20/80, to 0/100 in weight ratio, the first number referring to PVDF.

Thermal analysis was performed using a TA Instruments differential scanning calorimetry (DSC) Q100 with a Universal Analysis 2000. The samples were first annealed at 190 °C for 3 min to erase any thermal history, cooled to −70 °C at a cooling rate of 20 °C/min, and subsequently heated to 190 °C at a heating rate of 20 °C/min. The crystallization peak temperature (T_p) was obtained from the DSC cooling traces, while T_m was read from the second heating run.

A polarizing microscope (Olympus BX51) equipped with a first-order retardation plate and a temperature controller (Linkam THMS 600) was used to investigate the crystalline morphologies of PVDF/PBSA blends. Two different crystallization conditions, namely, one-step and two-step crystallization, were employed. For the one-step crystallization, PVDF/PBSA blends were quenched directly to T_c below T_m of PBSA from the homogeneous melt at a very fast cooling rate. For the two-step crystallization, PVDF/PBSA blends were cooled to the first crystallization temperature (T_{c1}) between T_ms of the two components for PVDF to crystallize and then cooled to the second crystallization temperature (T_{c2}) for PBSA to crystallize. The two-step crystallization consisted of the following two phase transitions, including from amorphous/amorphous to crystalline/amorphous state at T_{c1} and from crystalline/amorphous to crystalline/crystalline state at T_{c2}. PBSA must crystallize in the constrained space in the presence of pre-existing PVDF crystals whether one-step or two-step crystallization condition is used.

Results and Discussion

Miscibility Study of PVDF/PBSA Blends. DSC experiments showed that the glass transition temperature (T_g) of PVDF was −43.1 °C and that of PBSA was −44.8 °C at 20 °C/min after cooling from the crystal-free melt at 20 °C/min to −70 °C. Because of the proximity of T_gs of the two components, the miscibility of PVDF/PBSA blends could not be determined by measuring T_g of the blends conveniently as usual. Therefore, the miscibility of PVDF/PBSA blends was mainly evaluated by studying the crystallization peak temperature and the melting point temperature of the blends. Figure 1 shows the nonisothermal crystallization behavior of PVDF/PBSA blends at 20 °C/min from the homogeneous melt. A well-defined T_p was found at 132 °C for neat PVDF, which shifted to low-temperature range with increasing the PBSA content and decreased to 107 °C for 20/80 blend. However, the crystallization behavior of PBSA is a little complicated. T_p was found at around 50 °C for neat PBSA, which remained almost unchanged with increasing the PVDF content up to 50%. T_p of PBSA decreased to 39.7 °C for the 65/35 blend. With further increasing of the PVDF content, T_p of PBSA could not be found for 80/20 blend, probably due to its too small content in the blend and its weak crystallizability. Subsequent melting behavior of PVDF/PBSA blends was studied at 20 °C/min after they finished the nonisothermal crystallization as shown in Figure 2. Neat PVDF had a T_m at 165 °C, while neat PBSA showed a T_m at around 95 °C with a shoulder at 88.3 °C. Two main melting endotherms were found for PVDF/PBSA blends, corresponding to the T_ms of PVDF and PBSA, respectively. Double melting peaks, T_{m1} at low temperature and T_{m2} at high temperature, were found for PVDF in the blends, which shifted to low-temperature range

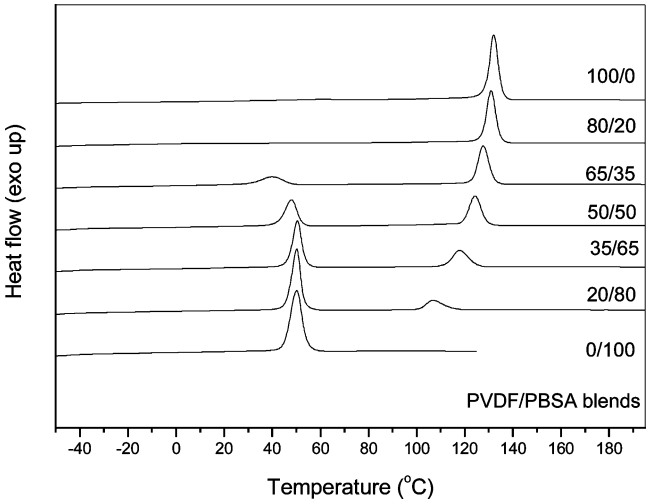

Figure 1. DSC cooling traces of PVDF/PBSA blends at 20 °C/min from the homogeneous melt.

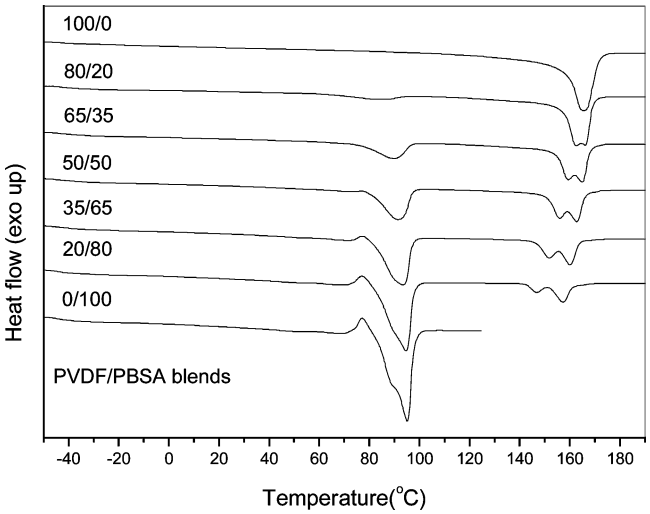

Figure 2. Subsequent melting behavior of PVDF/PBSA blends at 20 °C/min after cooling from the melt to −70 °C at 20 °C/min.

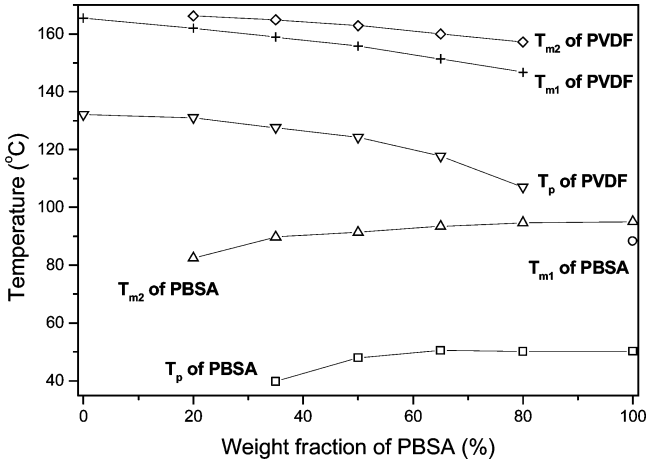

Figure 3. Phase behavior of PVDF/PBSA blends.

with increasing the PBSA content in the blends. T_{m1} shifted from 165 °C for neat PVDF to 146.7 °C for 20/80 blend. On the other hand, PBSA shows a well-defined T_m for almost all the samples except neat PBSA. T_m of PBSA shifted to 82.5 °C for 80/20 blend from 95 °C for neat PBSA.

Matkar and Kyu have recently developed a thermodynamically self-consistent theory to establish binary phase diagrams for two crystalline polymer blends by taking into consideration all interactions including amorphous−amorphous, crystal−amorphous, amorphous−crystal, and crystal−crystal interactions.[18] The Matkar and Kyu theory demonstrated the occurrence of the dual melting peaks in the binary crystalline polymer blends. The dual melting peaks reported in the present work are very clear and also in good agreement with the Matkar and Kyu theory.

For comparison, the values of T_p and T_m of PVDF/PBSA blends are summarized in Figure 3. T_p and T_m of the high-T_m component PVDF decreased significantly with increasing the PBSA content in the blends. T_m of the low-T_m component PBSA also decreased in the blends with increasing the PVDF content, while T_p of PBSA varied slightly. All the aforementioned results indicated the miscibility between PVDF and PBSA. The miscibility was further confirmed by the homogeneous melt of the blends by OM in the following section.

Crystalline Morphology of PBSA in PVDF/PBSA Blends. Crystalline morphology of miscible crystalline/crystalline polymer blends is of great interest from both academic and industrial viewpoints. The study of the crystalline morphology in these blend systems is not only concerned with the effects of blend composition and crystallization temperature but also related to the question of how the crystallinity of the one component affects the crystallization behavior of the other.

Figure 4 shows the spherulitic morphology of neat PVDF and PBSA. The size of PVDF spherulites at 150 °C was around 150 μm and that of PBSA at 75 °C had a similar value. Confined crystalline morphology of the low-T_m component PBSA in its miscible blends with PVDF was studied by OM under different crystallization conditions. As described in the experimental section, two different crystallization conditions, namely, one-step and two-step crystallization, were employed. Crystallization of PBSA in its miscible blends with PVDF was first studied under two-step crystallization condition. For the PVDF-rich blends, the high-T_m component PVDF spherulites at T_{c1} usually filled more or less the whole space, and the crystallization of the low-T_m component PBSA at T_{c2} had to occur in the confined space of the pre-existing PVDF spherulites. Figure 5 presents the crystallization process of PVDF/PBSA 50/50 blend as an

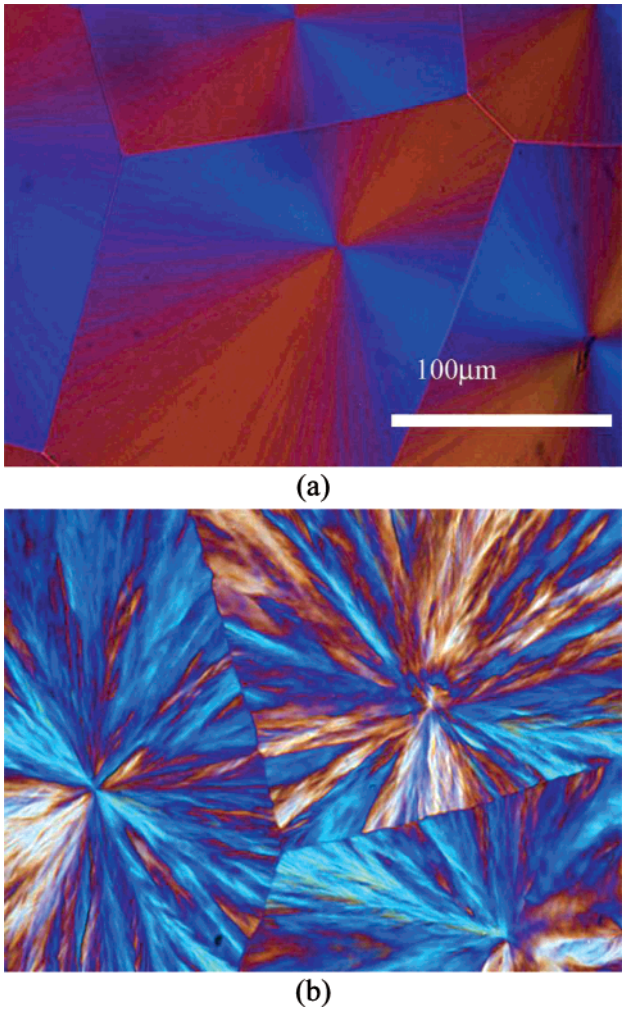

Figure 4. Spherulitic morphologies of neat components: (a) neat PVDF at 150 °C for 26 min and (b) neat PBSA at 75 °C for 60 min.

example. The sample was first crystallized at 148 °C (T_{c1}) to study the crystallization of PVDF and then cooled to 70 °C (T_{c2}) to study the crystalline morphology of PBSA. Figure 5a shows the PVDF spherulitic morphology after complete crystallization at 148 °C for 100 min. PBSA was still in the melt in this case, and the crystallization of PVDF corresponded to the transition from the fully amorphous to the amorphous/semicrystalline state. PVDF showed a typical birefringence pattern of negative spherulites with concentric extinction bands. PVDF spherulites remained more or less volume filling, although nonbirefringent space could be found at the spherulitic boundaries, indicating that most of PBSA was rejected into the interlamellar and interfibrillar regions of the PVDF spherulites during the crystallization process of PVDF and few of PBSA resided in the interspherulitic region. On lowering crystallization temperature to 70 °C, below T_m of PBSA, crystalline morphology of PBSA was studied in the presence of the pre-existing PVDF spherulites. Parts b and c of Figure 5 shows the crystallization of PBSA at 70 °C for 2 and 40 min, respectively. Commencement of the crystallization of PBSA occurred in the interspherulitic regions of the pre-existing PVDF spherulites by cooling the sample from 148 to 70 °C. The crystallization of PBSA continued to proceed in these interspherulitic domains, up to the point where they were more or less filled with PBSA crystallites (Figure 5b). PBSA could even crystallize inside the PVDF spherulites by prolonging the crystallization time. The crystallization of PBSA took place within the PVDF spherulites, which was confirmed by the change of the birefringent pattern

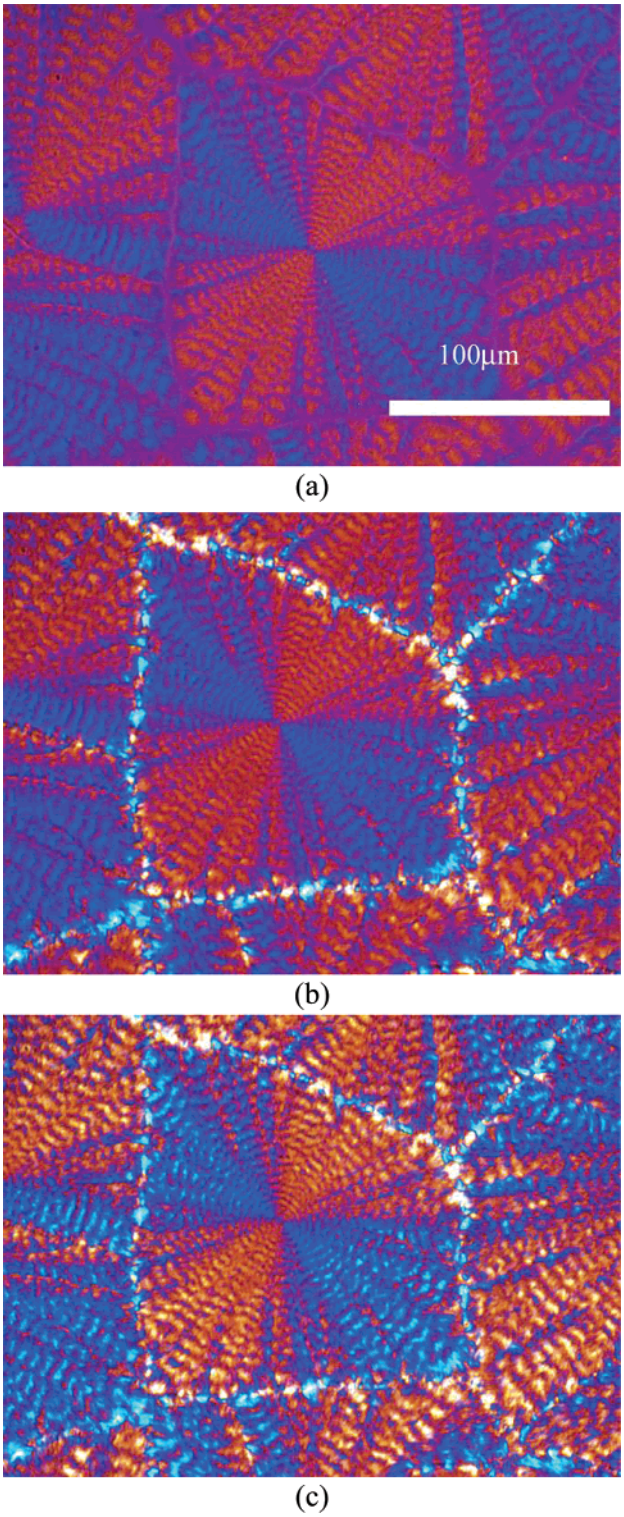

Figure 5. Crystallization of PBSA in 50/50 blend under two-step crystallization conditions: (a) crystallization of PVDF at 148 °C for 100 min, (b) crystallization of PBSA at 70 °C for 2 min, and (c) crystallization of PBSA at 70 °C for 40 min.

of the PVDF spherulites, i.e., the apparent increase of the brightness of the PVDF spherulites (Figure 5c). It should be noted that PBSA could not crystallize through spherulitic growth in the constrained space of the pre-existing PVDF spherulites, unlike the bulk crystallization of PBSA from the homogeneous melt. Only tiny crystals of PBSA were found within the spherulites or at the boundaries of the spherulites of the PVDF component. Such confined crystalline morphology was also found for other samples with different blend composition and the values of T_{c1} and T_{c2}. For instance, it was also found for 65/35 blend with T_{c1} ranging from 142 and 150 °C and T_{c2} ranging from 68 to 75 °C.

For the PVDF-poor blends, PVDF spherulites did not fill the whole space when the samples crystallized at high T_{c1} even for a very long time under two-step crystallization condition; therefore, PBSA may show different crystalline morphology from that for the PVDF-rich blends. Figure 6 demonstrates the crystallization of 20/80 blend under two-step crystallization. In Figure 6a, PVDF spherulites with sparse fibrils or concentric bands could be observed after the complete crystallization of PVDF at 146 °C (T_{c1}) for 400 min. At high T_{c1} even for a very long time, PVDF spherulites could not fill the whole space due to the depletion of the high-T_m component phase. On cooling the sample from T_{c1} to T_{c2}, PBSA could crystallize in the left space. Parts b, c, and d of Figure 6 represent a time sequence of the crystallization of PBSA at 75 °C after the complete crystallization of PVDF at 146 °C for 400 min. A spherulite of the PBSA phase first nucleated and continued to grow in the left space when the blend sample was cooled to 75 °C (Figure 6b). The PBSA spherulite with strong birefringence was brighter than those PVDF spherulites with weak birefringence. Both PVDF and PBSA showed spherulitic growth for 20/80 blend under two-step crystallization condition. It must be of great interest which kind of crystalline morphology will arise when the PBSA spherulite contacts the PVDF spherulites after longer crystallization time. With increasing crystallization time, the growth front of the PBSA spherulite reached the PVDF spherulites and continued to grow inside the spherulites instead of the termination of the growth (Figure 6c). The brightness of the PVDF spherulites increased in the region where PBSA crystallized and remained unchanged in the area where the growth front did not reach. The growth of the PBSA spherulite stopped until it impinged on another PBSA spherulite, which also penetrated the PVDF spherulites (Figure 6d). The penetration of the PVDF spherulites by the PBSA spherulites can be proved by the same discussion as in our previous works.[11,13] The increase in brightness obviously indicated that PBSA must crystallize inside the PVDF spherulites. Otherwise the brightness of the PVDF spherulites would have been constant if the PBSA spherulites grew only outside of the PVDF spherulites and just engulfed them as in the case of α and β forms of isotactic polypropylene.[17] Furthermore, the change of birefringence inside the PVDF spherulites also confirmed the penetration of them by the PBSA spherulites instead of forming a layered structure where the spherulites of the two components merely superposed on each other as two separate layers in a film. In the latter case, the image should be a result of the superposition of the birefringence patterns of PVDF and PBSA spherulites. Thus, the retardation would increase where they have the same birefringence and decrease where they have the opposite birefringence, resulting in the change of the color of the spherulites.[11,13] However, the experimental results demonstrated the increase of the brightness and the unchanged color of the PVDF spherulites after the PBSA spherulites crystallized inside them, indicating that the penetration process happened instead of two separate layers crystallization. It should also be noted that the shape of the growing PBSA spherulite remains circular although it penetrates the PVDF spherulites, indicating that the growth rate is almost the same for the left melt on the one hand and for the internal of the PVDF spherulites (Figure 6c). The same growth rate during the penetration process in PVDF/PBSA blend is different from the result in PES/PEO blend in previous work. In the PES/PEO blend, the growth rate of the PEO fibrils

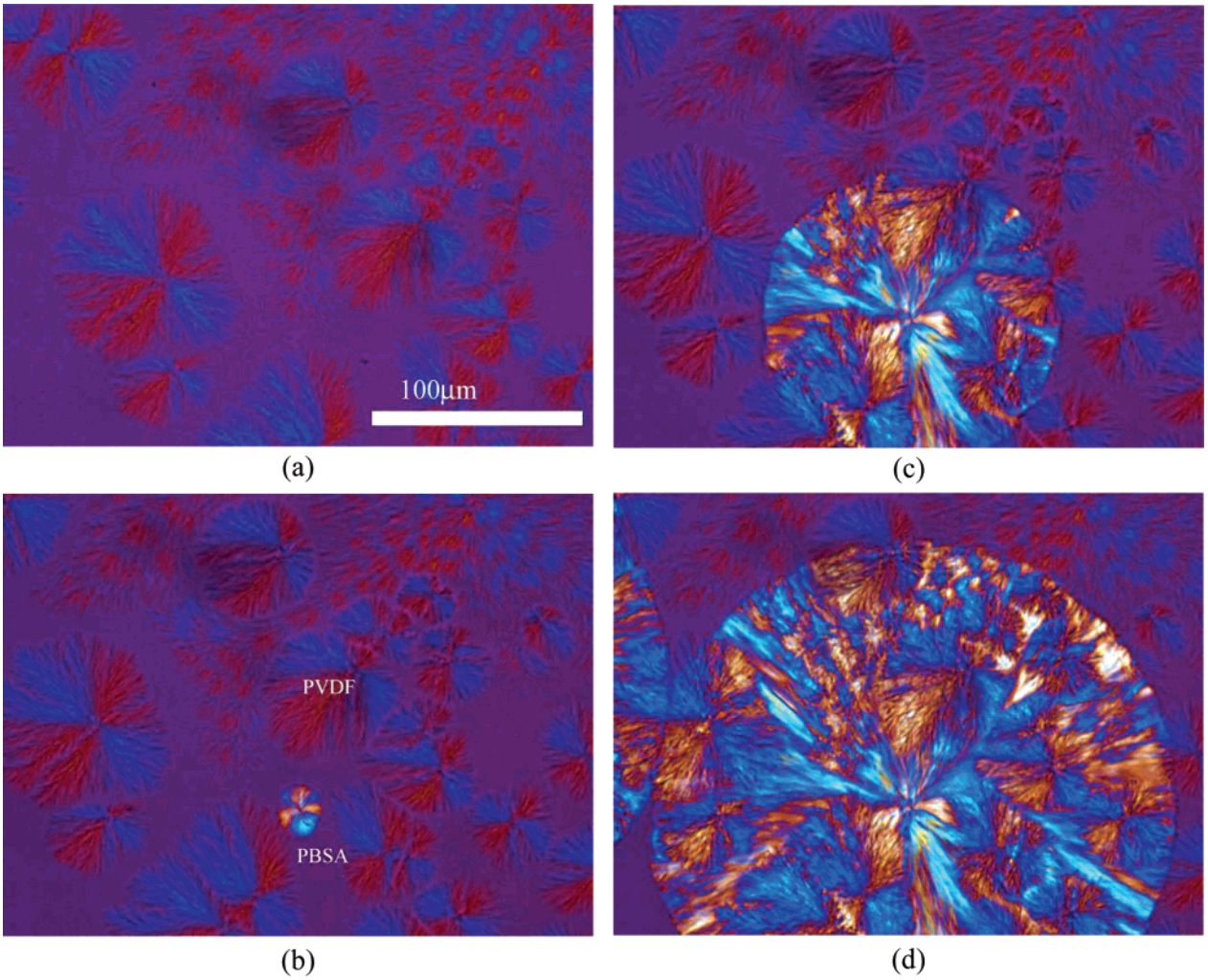

Figure 6. Formation process of interpenetrated spherulites in 20/80 blend under two-step crystallization conditions: (a) complete crystallization of PVDF at 146 °C for 400 min, (b) crystallization of 20/80 blend at 75 °C for 4 min, (c) process of interpenetration of PVDF spherulites by PBSA spherulite at 75 °C for 20 min, and (d) process of interpenetration of PVDF spherulites by PBSA spherulite at 75 °C for 32 min.

was faster inside the PES spherulite during the penetrating process than that for the left melt. The increase of the growth rate was attributed to the fact that the PEO content in the amorphous regions of the PES spherulite would be expected to be higher than the nominal melt concentration due to rejection of PEO from PES crystals. [13] In the case of PVDF/PBSA blend, the penetration process probably did not make a significant influence on the PBSA content inside and outside the PVDF spherulites, resulting in the growth rate of PBSA spherulite remains almost the same.

For comparison, the crystallization of 20/80 blend was also studied at 75 °C using one-step crystallization condition. It should be noted that PVDF always crystallized during the quenching process before T_c of PBSA was reached even at a maximum cooling rate of 100 °C/min. Therefore, the one-step crystallization process actually consisted of the following phase transitions. First, the phase transition from amorphous/amorphous to crystalline/amorphous state occurred during the quenching process from the homogeneous melt to T_c because PVDF crystallized while PBSA was still in the melt. Second, the phase transition from crystalline/amorphous to crystalline/crystalline state occurred at T_c after the crystallization of PBSA. Figure 7 demonstrates the crystallization process of 20/80 blend under one-step crystallization condition. The crystals of PVDF formed during the quenching process were more or less space filling; however, the size of PVDF crystals was suppressed significantly by the quenching process at 100 °C/min (Figure 7a). The PVDF crystals with weak birefringence were too small to be observed clearly by OM. With increasing crystallization time at 75 °C, several PBSA spherulites with strong birefringence were found to nucleate and continue to grow within the pre-existing PVDF crystals (Figure 7b). The growth of the PBSA spherulites proceeded with keeping the spherulitic shape until they impinged on other PBSA spherulites (Figure 7c). PBSA-type spherulites finally filled the whole sample. Such type of nucleation and spherulitic growth morphology were also found for other blend composition and T_c. For instance, 20/80 blend showed the similar morphology at T_c between 70 and 80 °C, and the 35/65 blend presented such crystalline morphology at T_c from 70 to 75 °C.

This type of nucleation and spherulitic growth have also been found in several binary miscible crystalline polymer blends, including PVDF/PBSU blends,[6] PBSU/PVCDC blends,[8−10] PEC/PLLA blends,[11,12] PBSA/PEO blends,[14] PBSU/PEO blends,[15] and PVDF/poly(3-hydroxybutyrate-*co*-hydroxyvalerate) (PHBV) blends.[16] The observation of the spherulitic growth of the low-T_m component is usually difficult in crystalline/crystalline polymer blends because it must crystallize in the matrix of the pre-existing crystals of the high-T_m component. Therefore, only tiny crystals of the low-T_m component can grow within the spherulites or at the boundaries of the spherulites of the high-T_m component. From the aforementioned studies and the related

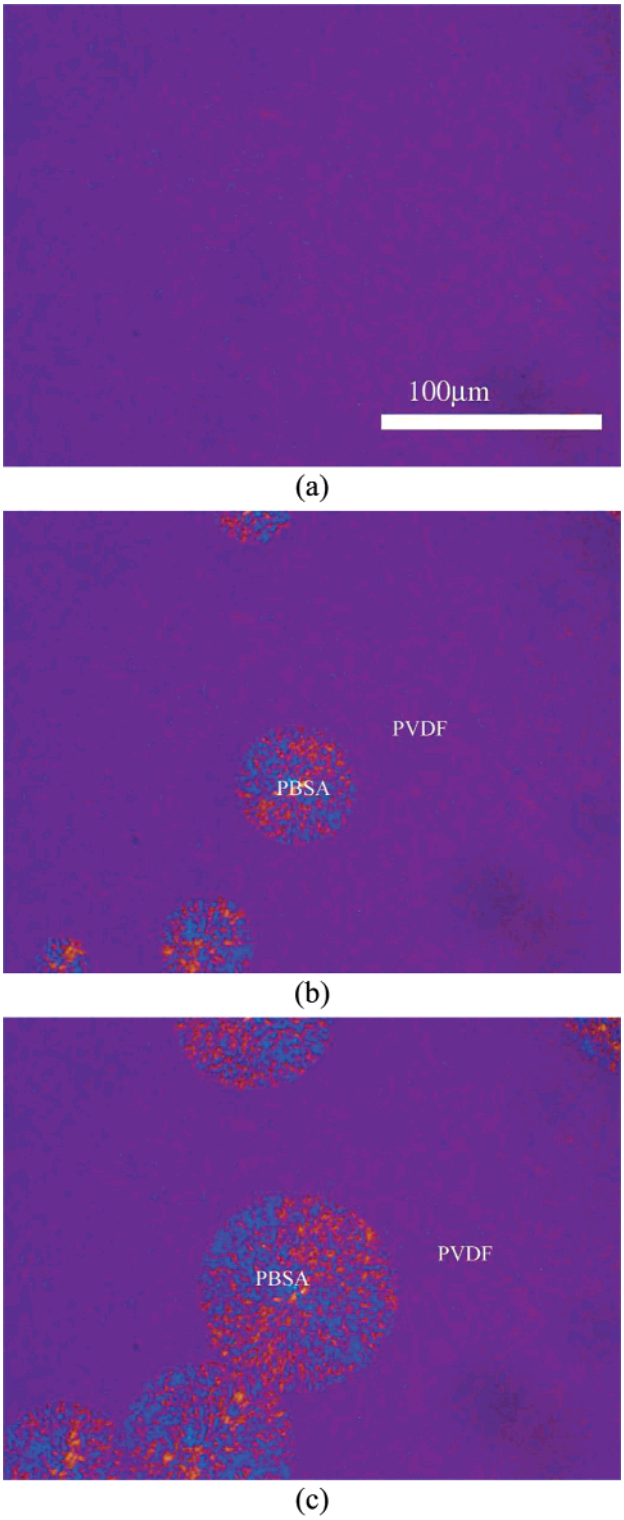

Figure 7. Nucleation and spherulitic growth of PBSA inside the PVDF spherulites in 20/80 blend under one-step crystallization conditions by quenching to 75 °C directly from the homogeneous melt. Crystallization times at 75 °C: (a) 0 min, (b) 6 min, and (c) 11 min.

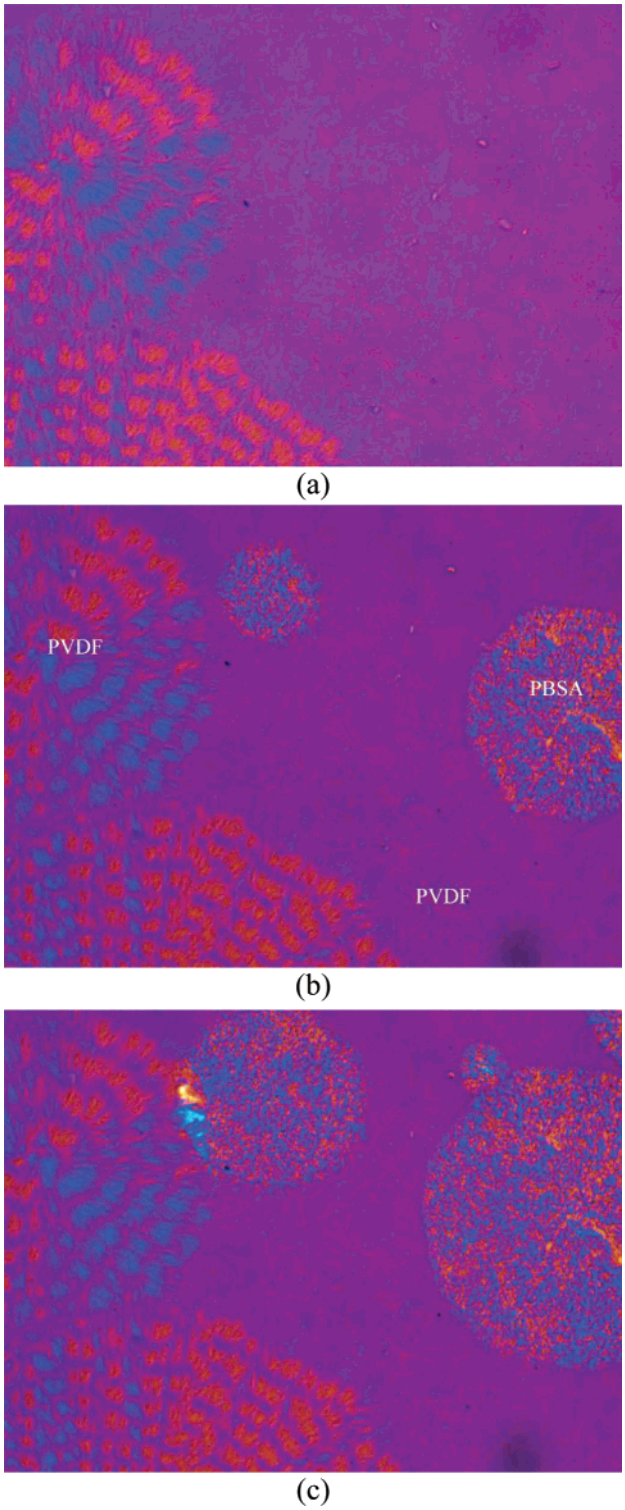

Figure 8. Crystallization of 35/65 blend under two-step crystallization conditions: (a) crystalline morphology at 75 °C for 0 min after the incomplete crystallization of PVDF at 146 °C for 120 min, (b) nucleation and spherulitic growth of PBSA inside the PVDF spherulites at 75 °C for 15 min, and (c) process of interpenetration of the PVDF spherulites by the PBSA spherulite at 75 °C for 20 min.

works, we propose that the possibility of the observation of the nucleation and spherulitic growth of the low-T_m component within the matrix of the pre-existing crystals of the high-T_m component may be related to the following two factors. One is the nucleation ability of the low-T_m component, and the other is the amount of its melt in the matrix of the pre-existing crystals of the high-T_m component. The lower nucleation ability and the higher amount of the melt of the low-T_m component favor the observation of its nucleation and spherulitic growth. In the case of 20/80 and 35/65 blends of this work, the nucleation ability of PBSA remained still very low at T_c ranging from 70 to 80 °C despite the presence of the PVDF crystals due to its low supercooling. Furthermore, the amount of the PBSA melt was high since PBSA was 65 and 80 wt % in these blends. On the basis of the aforementioned factors, PBSA nucleated and

grew within the pre-existing PVDF crystals for the PBSA-rich blends at high crystallization temperatures.

Finally, the crystallization of PBSA was studied under a specified crystallization condition by combining one-step and two-step crystallization conditions. We chose 35/65 blend as the model sample. The crystallization procedure was as follows. The sample was first crystallized at 146 °C (T_{c1}) for 120 min, which was not long enough for the high-T_m component PVDF to complete crystallization due to its slow crystallization rate. Under this condition some of PVDF crystallized through spherulitic growth, while the rest of PVDF was still in the melt. The sample was then quenched directly to 75 °C (T_{c2}) from 146 °C after the incomplete crystallization of PVDF for 120 min. During the quenching process, the rest of PVDF phase in the melt also crystallized and filled the rest of the whole sample before T_c of PBSA was reached. Figure 8a shows the crystalline morphology of PVDF formed through the above-mentioned procedure. Two large PVDF spherulites with obvious bands, similar to the crystalline morphology of PVDF at T_{c1} under two-step crystallization condition shown in Figure 5a, were found on the left of Figure 8a. They were formed through the crystallization at 146 °C for 120 min. Similar to the crystalline morphology in Figure 7a, the rest of Figure 8a was filled with tiny PVDF crystals, which was formed during the quenching process from 146 to 75 °C. With increasing crystallization time at 75 °C, two PBSA spherulites nucleated and continued to grow within the pre-existing PVDF crystals formed during the quenching process from T_{c1} to T_{c2} (Figure 8b), which was similar to the crystallization process of PBSA under one-step crystallization shown in Figure 7b. On further prolonging the crystallization time the PBSA spherulites would impinge on each other; furthermore, the growing PBSA spherulites would also reach the fixed banded PVDF spherulites. It must be of great interest what kind of crystalline morphology would occur when the spherulites from the same or different components impinge on each other. Figure 8c shows the crystalline morphology of 35/65 blend at 75 °C for 20 min. They stopped growing when the two PBSA spherulites impinged on each other on the up right part in Figure 8c. However, when one growing PBSA spherulite reached the fixed banded PVDF spherulite, it continued to grow inside the PVDF spherulite instead of growth termination. The brightness of the PVDF spherulite increased in the region where PBSA crystallized and remained unchanged in the region where PBSA did not crystallize. The growth front of the PBSA spherulite finally passed through the PVDF spherulite with further increasing the crystallization time. The results in Figure 8 demonstrated two different crystalline morphologies. One is that the growth of termination occurred when the PBSA spherulites impinged on each other. The other is that the interpenetration of PVDF spherulites by PBSA spherulites occurred when the growing PBSA spherulites reached the banded PVDF spherulites. It should also be noted that the shape of the growing PBSA spherulite remains almost circular although during the process of penetrating the PVDF spherulites, indicating that the growth rate is almost the same for the tiny PVDF crystals on the one hand and for the internal of the PVDF spherulites on the other hand (Figure 8c).

Conclusions

Miscibility and crystalline morphology of PVDF/PBSA were studied in this work by DSC and OM. PVDF/PBSA blends were miscible as evidenced by the depression of T_c and T_m of each component with increasing the content of the other component and the homogeneous melt. Crystalline morphology of PBSA was studied extensively by changing blend composition and crystallization conditions. Depending on blend composition and crystallization conditions, there are mainly three different types of crystalline morphologies. The various crystalline morphologies are expected to play a significant role on the thermal, mechanical, and other properties of PVDF/PBSA blends.

Acknowledgment. This work was financially supported by the National Natural Science Foundation, China (Grant No. 20504004), Program for New Century Excellent Talents in University, and the projects of Polymer Chemistry and Physics, BMEC (Grant Nos. XK100100433 and XK100100540).

References and Notes

(1) Avella, M.; Martuscelli, E. *Polymer* **1988**, *29*, 1731.
(2) Marand, H.; Collins, M. *ACS Polym. Prepr.* **1990**, *31*, 552.
(3) Chen, H. L.; Wang, S. F. *Polymer* **2000**, *41*, 5157.
(4) Liu, A. S.; Liau, W. B.; Chiu, W. Y. *Macromolecules* **1998**, *31*, 6593.
(5) Penning, J. P.; Manley, R. St. J. *Macromolecules* **1996**, *29*, 84.
(6) Lee, J. C.; Tazawa, H.; Ikehara, T.; Nishi, T. *Polym. J.* **1998**, *30*, 327.
(7) Blümm, E.; Owen, A. J. *Polymer* **1995**, *36*, 4077.
(8) Lee, J. C.; Tazawa, H.; Ikehara, T.; Nishi, T. *Polym. J.* **1998**, *30*, 780.
(9) Ikehara, T.; Nishi, T. *Polym. J.* **2000**, *32*, 683.
(10) Terada, Y.; Ikehara, T.; Nishi, T. *Polym. J.* **2000**, *32*, 900.
(11) Hirano, S.; Nishikawa, Y.; Terada, Y.; Ikehara, T.; Nishi, T. *Polym. J.* **2002**, *34*, 85.
(12) Ikehara, T.; Nishikawa, Y.; Nishi, T. *Polymer* **2003**, *44*, 6657.
(13) Qiu, Z.; Ikehara, T.; Nishi, T. *Macromolecules* **2002**, *35*, 8251.
(14) Ikehara, T.; Kimura, H.; Qiu, Z. *Macromolecules* **2005**, *38*, 5104.
(15) Qiu, Z.; Ikehara, T.; Nishi, T. *Polymer* **2003**, *44*, 2799.
(16) Qiu, Z.; Fujinami, S.; Komura, M.; Nakajima, K.; Ikehara, T.; Nishi, T. *Polymer* **2004,** *45*, 4515.
(17) Varga, J. *J. Mater. Sci.* **1992**, *27*, 2557.
(18) Matkar, R.; Kyu, T. *J. Phys. Chem. B* **2006**, *110*, 16059.